Coherence dynamics of a two-mode Bose-Einstein condensate coupled with the environment

Yixiao Huang,[1] Qing-Shou Tan,[1] Li-Bin Fu,[2] and Xiaoguang Wang[1,*]

[1]*Zhejiang Institute of Modern Physics, Department of Physics, Zhejiang University, Hangzhou 310027, China*

[2]*National Key Laboratory of Science and Technology on Computation Physics, Institute of Applied Physics and Computational Mathematics, Beijing 100088, China*

(Received 29 January 2013; published 26 December 2013)

We investigate the coherence dynamics of a two-mode Bose-Einstein condensate coupled with the environment in the mean-field approximation. We give an analytical result of the time-average coherence in the absence of system-environment coupling, and find that the time-average coherence attains its maximum value at the critical point which corresponds to the boundary between the self-trapping regime and the Josephson oscillation regime. The effect of noise on dynamical coherence is also considered by analyzing the couplings of the condensate to the environment. With the first kind of coupling, the coherence finally stabilizes at a fixed value. Meanwhile, we show that the presence of the noise can even enhance the coherence for some particular interaction. With the second kind of coupling as collisional dephasing, the noise leads a sudden transition of the coherence which then subjects to an exponential decay.

DOI: 10.1103/PhysRevA.88.063642 PACS number(s): 03.75.Gg, 03.75.Kk

I. INTRODUCTION

The physics of Bose-Einstein condensates (BECs) in a double-well potential has made enormous progress in the last decade, as it is an excellent model system for a variety of quantum fields such as condensed matter physics or nonlinear dynamics [1–6]. With rapid experimental progress in manipulation of cold atoms, almost every parameter can be tuned in the experiment. For example, the intracomponent and intercomponent interaction constants can be controlled by tuning the atomic s-wave scattering length, and also the energy bias between the two wells [7–11]. By tuning the parameters, the BECs in a double well exhibit several fascinating phenomena, such as quantum tunneling, self-trapping, and coherent oscillations [12–29]. A most prominent feature of its tunneling and coherence is the nonlinear dynamics arising from the atom-atom interaction. Recently, many theoretical works showed that the coherence between the two wells exhibited different behaviors in the Fock regime, Josephson regime, and Rabi regime [30,31].

In the past few years, phenomena such as self-trapping and Josephson oscillation were observed in the experiments [5]. However, in the present experimental conditions, the condensates usually coexist with noncondensed thermal clouds and atom loss is also unavoidable; it means the condensate should be regarded as an open system coupled with the environment. Many theoretical works have investigated the effect of the noise on the BECs in the double-well condensate, and found it leads to the decay of quantum self-trapping [32], decoherence [33–35], particle loss [36–39], and dephasing [40–43]. The phenomenon of the dephasing has even been observed in experiments [44,45]. Recently, it was shown that the maximum pin squeezing can be reached in the presence of particle losses [39]. Researchers even found that the dissipations can enhance the quantum coherence between the two wells for some particular conditions [46,47]. Hence, the characterization of the double-well potential coupled with the environment is interesting. Treating the environment as a Markovian reservoir, the dynamics of the condensate atoms could be characterized by the master equations [48–50]. As we know, the different types of coupling with the environment have different effect on the dynamics of the BECs. In Ref. [51], it is shown that the different kinds of BEC-environment coupling lead to different final population imbalance of the BEC in a double well. As we know, the relative phase and the degree of coherence are believed to affect the dynamical properties of BECs in the double well [31], and it is worthwhile to study the coherence dynamics. In this work, we focus on the dynamics of coherence between the two wells for different kinds of BEC-environment coupling.

In this paper, we study the effect of BEC-environment coupling on the dynamics of a BEC in a double-well potential. We investigate the dynamics of coherence between the two wells within a mean-field framework. For the closed system, i.e., no coupling between the system and the environment, we give an analytical result of the time-average coherence and show that it attains maximum value at the critical point which corresponds to the boundary between the Josephson oscillation and self-trapping regimes. We also study the dynamics of coherence under two different kinds of BEC-environment coupling. With the first kind of coupling dominating, the coherence finally stabilizes at a fixed value. We also show the coherence enhancement in the presence of noise under some specific conditions. For the second kind of condensate-environment coupling such as collisional dephasing, we find that the noise induces a sudden transition of the coherence in the process of evolution, and then the coherence is subject to an exponential decay.

The paper is organized as follows. In Sec. II, we give a brief discussion of the two-well potential system in the mean-field approximation and study the dynamics of the coherence in the absence of condensate-environment coupling. Then, in Sec. III, we discuss the coherence under two different kinds of the condensate-environment coupling. Finally, a summary is given in Sec. IV.

*xgwang@zimp.zju.edu.cn

 ©2013 American Physical Society

II. MODEL

We consider two coupled BECs in a double well; the system can be described by the Hamiltonian [13,14]

$$\hat{H} = \hat{H}_L + \hat{H}_R + \hat{H}_{\rm int} + \hat{H}_{\rm las}, \tag{1}$$

where

$$\hat{H}_L = \omega_L \hat{a}_L^\dagger \hat{a}_L + \frac{U_{LL}}{2} \hat{a}_L^\dagger \hat{a}_L^\dagger \hat{a}_L \hat{a}_L,$$
$$\hat{H}_R = \omega_R \hat{a}_R^\dagger \hat{a}_R + \frac{U_{RR}}{2} \hat{a}_R^\dagger \hat{a}_R^\dagger \hat{a}_R \hat{a}_R,$$
$$\hat{H}_{\rm int} = U_{LR} \hat{a}_L^\dagger \hat{a}_R^\dagger \hat{a}_R \hat{a}_L,$$
$$\hat{H}_{\rm las} = \frac{v}{2} (\hat{a}_L^\dagger \hat{a}_R e^{-i\Delta t} + \hat{a}_R^\dagger \hat{a}_L e^{i\Delta t}).$$

Here, $H_{L,R}$ represents the evolution of atoms in the left and right wells, respectively, $H_{\rm int}$ represents the interaction between atoms in the left and right wells due to collisions, and $H_{\rm las}$ represents the coupling between the two wells induced by the laser detuned by Δ from the Raman resonance. $\hat{a}_R^{(\dagger)}$ and $\hat{a}_L^{(\dagger)}$ are the bosonic annihilation (creation) operators for the right and left wells, respectively. The parameter $U_{LL,RR}$ is the effective self-interaction of atoms, v is the effective Rabi frequency which describes the coupling between two wells, and U_{LR} is the cross interaction. In the following, we consider the condensates situated in the individual wells are merely weakly coupled, i.e., the cross interaction U_{LR} is much smaller than the self-interaction $U_{LL,RR}$, therefore the interaction $H_{\rm int}$ can be neglected. In this work, we focus on the case that the atoms condensate in a symmetric double well, then the Hamiltonian (1) (with constant terms dropped) can be remarkably simplified as [1,12,52]

$$\hat{H} = \frac{c}{2N} (\hat{a}_R^\dagger \hat{a}_R - \hat{a}_L^\dagger \hat{a}_L)^2 + \frac{v}{2} (\hat{a}_R^\dagger \hat{a}_L + \hat{a}_L^\dagger \hat{a}_R), \tag{2}$$

where $2c/N = U_{LL} = U_{RR}$. The detailed derivation of this Hamiltonian is provided in the Appendix.

If the particle number is sufficiently large, the system can be well described in a mean-field approximation. For such an approximation, the dynamics of the system is described by a classical Hamiltonian $H = \langle \Psi_{GP} | \hat{H} | \Psi_{GP} \rangle / N$, in which $|\Psi_{GP}\rangle = 1/\sqrt{N!} (a_R \hat{a}_R^\dagger + a_L \hat{a}_L^\dagger)^N |0\rangle$ is the coherent superposition state and N is the particle number. The coefficients a_R and a_L are the probability amplitudes of atoms in the right and left wells, respectively. Without loss of generality, a_R and a_L can be represented as $|a_R| e^{i\theta_R}$ and $|a_L| e^{i\theta_L}$, respectively.

By introducing the population difference $s = |a_L|^2 - |a_R|^2$ and the relative phase $\theta = \theta_R - \theta_L$. The classical Hamiltonian can be reduced to [2,3,12]

$$H = \frac{c}{2} s^2 + v\sqrt{1 - s^2} \cos\theta, \tag{3}$$

where s and θ are canonical conjugates with $\dot{s} = -\partial H/\partial\theta$, $\dot{\theta} = \partial H/\partial s$. According to the expression of the Hamiltonian (3), their equations of motions are [2,3,12]

$$\dot{s} = v\sqrt{1 - s^2} \sin\theta, \quad \dot{\theta} = cs - \frac{vs}{\sqrt{1 - s^2}} \cos\theta. \tag{4}$$

We first investigate the dynamics of the coherence in the absence of BEC-environment coupling, which can be characterized by one element of the reduced single-particle density matrix $|\rho_{12}|$ with the definition $\rho_{i,j}^{(1)} = \frac{1}{N} \langle \hat{a}_i^\dagger \hat{a}_j \rangle$, with the mode indices $i, j = R, L$. Clearly, RR and LL represent the population in the right and left wells, respectively. According to Eq. (4), the equation of motion for $|\rho_{12}|$ is

$$\frac{d|\rho_{12}|}{dt} = \frac{d\sqrt{1 - s^2}}{2\,dt}. \tag{5}$$

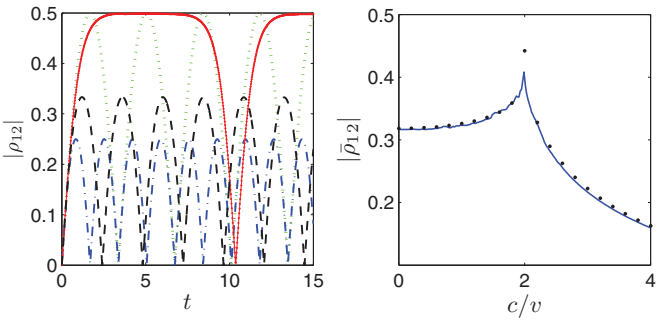

FIG. 1. (Color online) For initial condition $s = 1$ and relative phase $\theta = 0$, coherence $|\rho_{12}|$ evolves with time. Dotted green, solid red with dots, black dashed, and dashed-dotted blue lines correspond to $c/v = 1,2,3,4$, respectively (left column). Time average of coherence $|\bar{\rho}_{12}|$ as a function of parameter c/v (right column). The circles are for analytic formula (11) and the blue line is for numerical simulation.

In Fig. 1, we plot the time evolution of $|\rho_{12}|$ and its time average $|\bar{\rho}_{12}|$ with the initial condition $\theta = 0$ and $s = 1$. It can be found that $|\rho_{12}|$ oscillates with different periods for different interaction strengths c/v. When $c/v < 2$, the amplitude of the oscillation is independent of the interaction strength and equal to 0.5, meanwhile the period decreases with increasing c/v. However, when $c/v > 2$, the amplitude decreases with increasing the interaction and the period increases with increasing the interaction. Hence, $|\bar{\rho}_{12}|$ will increase with increasing interaction in the regime of $c/v < 2$, while it will decrease with increasing interaction when $c/v > 2$.

The above phenomenon can be well understood by analyzing the classical Hamiltonian system on the phase space. In Fig. 2, we plot the trajectories in phase space for two different parameters. For the classical Hamiltonian system (3), we can

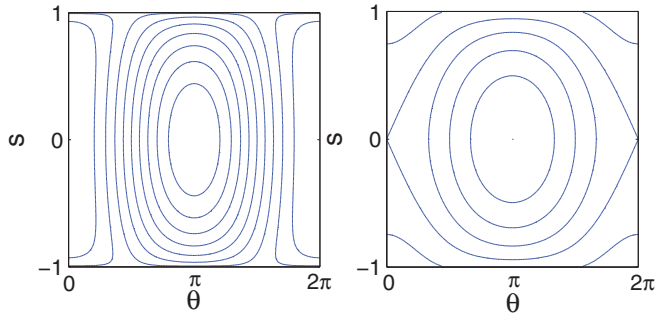

FIG. 2. (Color online) Trajectories on the phase space of the classical Hamiltonian system with $c = v$ (left column) and $c = 3v$ (right column).

obtain the period T of a given trajectory from the integral [17]

$$T = -\oint 1/(\partial H/\partial\theta)ds, \tag{6}$$

and the time average $|\rho_{12}|$ for it from

$$|\bar{\rho}_{12}| = (1/T)\oint |\rho_{12}|(dt/d|\rho_{12}|)d|\rho_{12}|, \tag{7}$$

in which the integral path is along the trajectory. For the trajectory with initial atoms condensate in the left well (i.e., $s = 1$), we have $H(s = 1) = c/2$. Thus, from Eqs. (3) and (4), we obtain

$$T = \begin{cases} \frac{4}{\sqrt{4v^2-c^2}} K\left(\frac{c^2}{c^2-4v^2}\right), & c < 2v \\ \frac{-4}{\sqrt{c^2-4v^2}} \mathrm{Im}\left[K\left(\frac{c^2}{c^2-4v^2}\right)\right], & c > 2v \end{cases} \tag{8}$$

which agree well with the result in Ref. [52]. In the above equation, $K(m)$ is the complete elliptic integral of the first kind and defined as

$$K(m) = \int_0^{\pi/2} \frac{d\theta}{\sqrt{(1 - m\sin^2\theta)}}. \tag{9}$$

According to Eqs. (5) and (7), we have

$$|\bar{\rho}_{12}| = \begin{cases} \frac{1}{T}\int_{-1}^{1} \frac{ds}{\sqrt{4v^2-c^2(1-s^2)}}, & c < 2 \\ \frac{1}{T}\int_{\sqrt{1-(2v/c)^2}}^{1} \frac{ds}{\sqrt{4v^2-c^2(1-s^2)}}, & c > 2v. \end{cases} \tag{10}$$

Here, we have used the relation $\cos\theta = c\sqrt{1-s^2}/2v$. After some elaboration, the time average of $|\rho_{12}|$ can be obtained and given by

$$|\bar{\rho}_{12}| = \begin{cases} \sqrt{4v^2-c^2}\ln\left(\frac{2v+c}{2v-c}\right)/\left[4K\left(\frac{c^2}{c^2-4v^2}\right)c\right], & c < 2v \\ \sqrt{c^2-4v^2}\ln\frac{c-2v}{c+2v}/\left\{4\,\mathrm{Im}\left[K\left(\frac{c^2}{c^2-4v^2}\right)\right]c\right\}, & c > 2v. \end{cases} \tag{11}$$

As shown in Fig. 1(b), the theoretical results of the time-average coherence $|\bar{\rho}_{12}|$ (11) is confirmed by numerical results obtained by numerically solving Eq. (4) with Runge-Kutta algorithm. It is clearly seen that $|\bar{\rho}_{12}|$ attains its maximum value at the critical point $c/v = 2$, which corresponds to the boundary between the Josephson oscillation regime and self-trapping regime. In Fig. 1(b), we can also see that near the transition point, there is a divergency between the numerical and analytical results: it is because the critical behavior is closely related to the separatrix of the Hamiltonian. Near the separatrix, the period of the trajectory diverges to infinity as a function of the relative deviation of the energy from the separatrix energy.

III. EFFECT OF NOISE ON COHERENCE

Now, we consider the condensate atoms coupled with the environment. In this work, we consider the effect of two types of noise on the two-mode dynamics with the master equation takes the form [41,42]

$$\frac{\partial}{\partial t}\rho = -i[H,\rho] - 2\Gamma_x[S_x,[S_x,\rho]] - 2\Gamma_z[S_z,[S_z,\rho]], \tag{12}$$

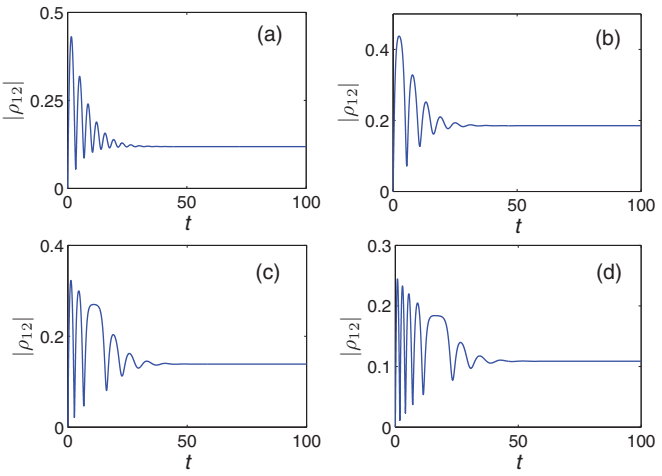

FIG. 3. (Color online) Coherence $|\rho_{12}|$ as a function of time, starting from the condensate prepared in the left well with (a) $c = v$, (b) $c = 2v$, (c) $c = 3v$, (d) $c = 4v$. The decoherence rate is chosen as $\Gamma_x = 0.05v$.

where ρ is the density matrix of system states, $S_x = \frac{\hat{a}_R^\dagger\hat{a}_L + \hat{a}_R\hat{a}_L^\dagger}{2}$, $S_z = \frac{\hat{a}_R^\dagger\hat{a}_R - \hat{a}_L^\dagger\hat{a}_L}{2}$, and $\Gamma_{x,z}$ is the decoherence rate. In the following, we will investigate the coherence between the two wells, which is given by one element of the reduced single-particle density matrix $|\rho_{12}|$.

A. Case of $\Gamma_z = 0$

To start with, we consider the case of $\Gamma_x \neq 0$ and $\Gamma_z = 0$. This situation may be implemented, e.g., by a stochastic modulation of the potential barrier between the wells [41,42]. According to Eq. (12), the equations of motion for the reduced single-particle density matrix are

$$\dot{\rho}_{11} = -\dot{\rho}_{22} = -\Gamma_x(\rho_{11} - \rho_{22}) + iv(\rho_{12} - \rho_{21})/2, \tag{13}$$

$$\dot{\rho}_{12} = i/2(v - 2c\rho_{12})(\rho_{11} - \rho_{22}) - \Gamma_x(\rho_{12} - \rho_{21}). \tag{14}$$

The dynamics of coherence is illustrated in the numerical results of Fig. 3, where we plot the dynamics of the coherence as a function of time for various interactions with the condensates initially in the left well and the decoherence rate $\Gamma_x = 0.05v$. Clearly, the decoherence decreases the amplitude of oscillations in the $|\rho_{12}|$ first and finally induces $|\rho_{12}|$ stabilized at a fixed value independent of the time, which indicates that this kind of the coupling can not lead to the coherence vanishing. In this figure, we also note that the final fixed values of $|\rho_{12}|$ are dependent on the interaction strength c/v, i.e., the different interaction strengths determine the different final fixed values.

In order to investigate the relation between the final fixed value of $|\rho_{12}|$ and the interaction strength c/v, in Fig. 4 we plot the fixed value of $|\rho_{12}|$ as a function of c/v at $t = 100$. For simplicity, in the following we denote the final fixed value of $|\rho_{12}|$ as $|\rho_{12}|_\infty$. As shown in Fig. 4, $|\rho_{12}|_\infty$ shows plenty of features. First, one can see that the values of $|\rho_{12}|_\infty$ increase with increasing c/v first and then attain maximum values at some points of c/v. For the small decoherence rate

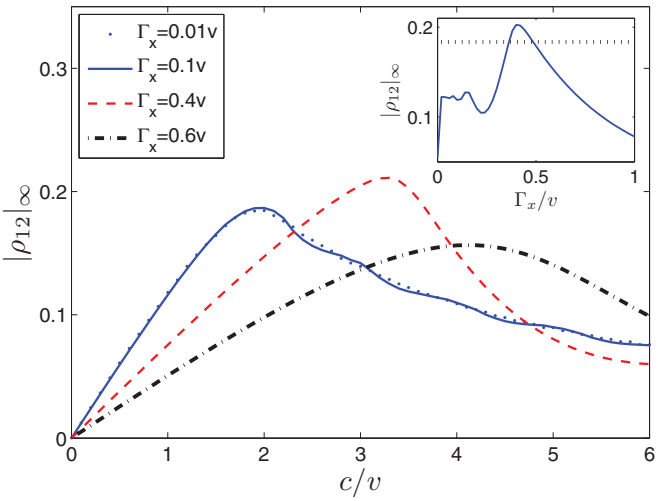

FIG. 4. (Color online) Coherence $|\rho_{12}|_\infty$ as a function of c/v with different decoherence rate. The inset shows $|\rho_{12}|_\infty$ as a function of Γ/v with the interaction strength $c/v = 3.5$. The horizontal dashed line is the numerical result of time-average coherence $|\bar{\rho}_{12}|$ with $\Gamma_x = 0$ and $c/v = 3.5$.

(i.e., $\Gamma_x = 0.01v$, $0.1v$), the results of $|\rho_{12}|_\infty$ are nearly the same, and the points which correspond to the maximum values of the coherence are close to $c/v = 2$. While for the large decoherence rate (i.e., $\Gamma_x = 0.4v$, $0.6v$), it can be found that the points corresponding to the maximum values of $|\rho_{12}|_\infty$ are far away from the value of $c/v = 2$. It means the effect of the system-environment coupling shifts the transition values. In Fig. 4 , we can also find that at some values of c/v, $|\rho_{12}|_\infty$ for the large Γ_x are larger than that for the small Γ_x . As shown in the inset of Fig. 4, $|\rho_{12}|_\infty$ as a function of Γ_x is plotted with interaction strength $c/v = 3.5$. It can be found that in some regimes, $|\rho_{12}|_\infty$ increases with the coupling strength increasing. Moreover, we can see that in some regimes, the values of $|\rho_{12}|_\infty$ for $\Gamma_x > 0$ even larger than $|\bar{\rho}_{12}|$ for $\Gamma_x = 0$. It means that the presence of BEC-environment coupling can enhance the coherence for some particular interaction strength.

On the other hand, the decoherence may also influence the dynamics of the population difference between the two wells. According to Eq. (13), the equation of motion for the population difference is given by

$$\dot{s} = -2\Gamma_x(\rho_{11} - \rho_{22}) + iv(\rho_{12} - \rho_{21}). \tag{15}$$

As shown in Fig. 5, it can be clearly seen that when c/v is small ($c/v < 2$), s oscillates nearly symmetrically in the whole plane. This phenomenon is similar to the case of N-particle oscillation in which a "damping" oscillation is apparent [52]. While c/v is bigger ($c/v > 2$), s oscillates in the half plane first and some time later it equals to zero which indicates that the decoherence destroys the quantum tunneling or self-trapping after a few cycles of evolution. It is much different from the results of the N-particle case without decoherence in which the population difference s only oscillates in a half plane and for intermediate times stabilizes at a fixed value [52].

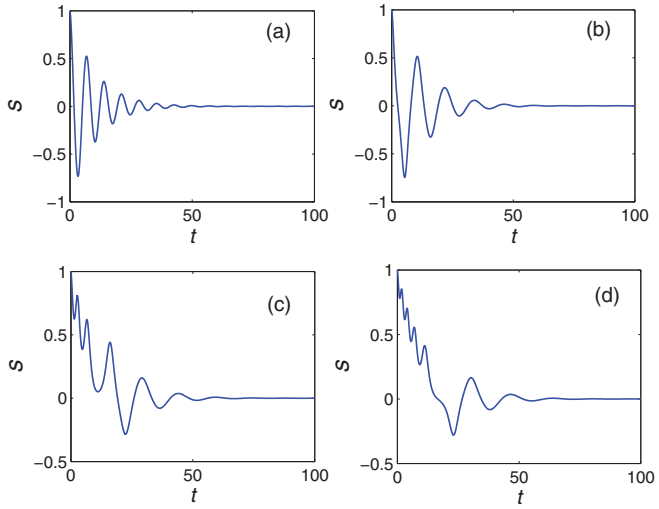

FIG. 5. (Color online) Time evolution of the population difference (15) for different interaction strengths (a) $c = v$, (b) $c = 2v$, (c) $c = 3v$, (d) $c = 4v$. The initial condition is the condensate in the left well and the decoherence rate chosen is $\Gamma_x = 0.05v$.

B. Case of $\Gamma_x = 0$

Next, we consider the case of $\Gamma_x = 0$: for this kind of coupling, it may be caused by collisions with thermal atoms. According to Eq. (12), we get the equations of motion for the elements of the single-particle density matrix:

$$\dot{\rho}_{11} = -\dot{\rho}_{22} = iv(\rho_{12} - \rho_{21})/2, \tag{16}$$

$$\rho_{12} = -2\Gamma_z\rho_{12} + i(v - 2c\rho_{12})(\rho_{11} - \rho_{22})/2. \tag{17}$$

For such a noise, it is usually interpreted as a collisional dephasing.

In Fig. 6, we plot the dynamics of $|\rho_{12}|$ with different interactions by numerically solving Eqs. (16) and (17). It

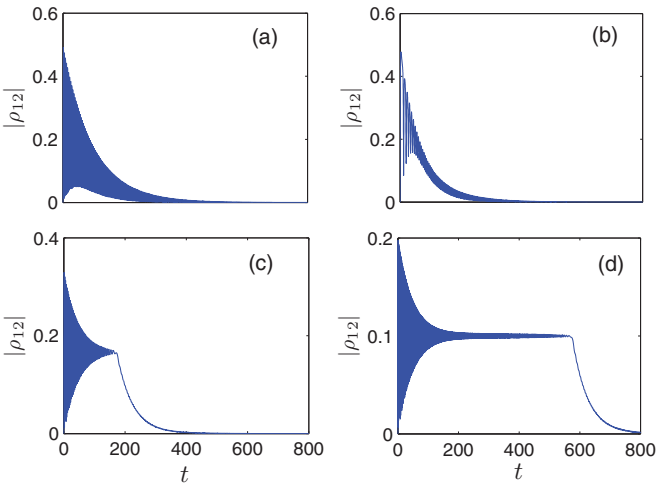

FIG. 6. (Color online) Coherence $|\rho_{12}|$ as a function of time with (a) $c = v$, (b) $c = 2v$, (c) $c = 3v$, (d) $c = 5v$. The initial condition is the condensate in the left well and the decoherence rate chosen is $\Gamma_z = 0.01v$.

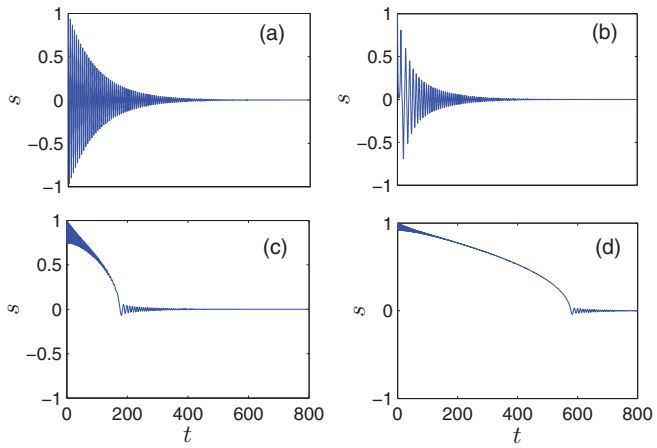

FIG. 7. (Color online) Time evolution of the population difference for different interaction strengths (a) $c = v$, (b) $c = 2v$, (c) $c = 3v$, (d) $c = 5v$. The initial condition is the condensate in the left well and the decoherence rate chosen is $\Gamma_z = 0.01v$.

can be found that the coherence finally vanishes under the noise. However, we notice that the behaviors of $|\rho_{12}|$ in the evolutionary process are obviously different for different interactions. For the weak interaction, as shown in Figs. 6(a) and 6(b), the noise decreases the amplitude of oscillations of $|\rho_{12}|$ first and finally spoils the coherence. For strong interaction, as shown in Figs. 6(c) and 6(d), the amplitude of oscillations of $|\rho_{12}|$ decreases first and then it oscillates symmetrically along a fixed value. After some time, the coherence $|\rho_{12}|$ exhibits a sudden decreasing and then decays as a function of exponent.

For the above phenomenon, it can be understood from an analysis on the time evolution of the population difference. In Fig. 7, we plot the population difference for different c/v. From this figure, we can see clearly that for a small c/v [i.e., Figs. 7(a) and 7(b)], the population difference s oscillates between 1 and -1 with its amplitude decreasing with the time evolution. For a large c/v, s oscillates in a half plane [Figs. 7(c) and 7(d) in the positive plane] first, then it oscillates symmetrically along the value $s = 0$ with a small amplitude. According to Eq. (17), we can find that when $s = 0$, the equation of motion for ρ_{12} reduces to

$$\dot{\rho}_{12} = -2\Gamma_z \rho_{12}. \tag{18}$$

Then, we have

$$|\rho_{12}(t)| = e^{-2\Gamma_z t}|\rho_{12}(t_c)|, \tag{19}$$

where t_c is the time when $s = 0$. According to Eq. (19), we note that coherence exhibits an exponential decay which is shown in Figs. 6(c) and 6(d). From the above result, we know the coherence has a close relation with the population difference. It is shown that for the strong interaction, the coherence of the system will always oscillate symmetrically as long as the atomic population is nonequilibrium between the two wells; when the atomic population is balanced between the two wells, the coherence presents a sudden transition and subjects to an exponential decay.

IV. CONCLUSION

We have analyzed the dynamics of a Bose-Einstein condensate in a double-well potential in the frame of the mean-field approximation. We investigated the dynamics of the coherence between the two wells and gave an analytical result of time-average coherence in the absence of the BEC-environment coupling. We give an analytical result of the time-average coherence and show that it attains maximum value at the critical point which corresponds to the boundary between the Josephson oscillation and self-trapping regimes.

We also studied the dynamics of coherence under noise. By numerically solving the master equations with condensate operators which are characterized by S_x and S_z, we showed that under the first kind of the coupling S_x, the coherence finally stabilizes at a fixed value, and found that the presence of BEC-environment coupling can even enhance the coherence for some particle interaction strength. We also showed that the points which correspond to the maximum value of $|\rho_{12}|_\infty$ are far away from $c/v = 2$, which indicates the effect of the system-environment coupling shifts the transition values. When the second kind of coupling S_z dominates, the noise destroys the coherence. However, for the strong interaction strength c/v, $|\rho_{12}|$ exhibits a sudden transition after some time and then subjects to an exponential decay.

ACKNOWLEDGMENTS

X.W. acknowledges support from the NFRPC with Grant No. 2012CB921602 and NSFC with Grants No. 11025527 and 10935010. L.-B.F. acknowledges support from the National Nature Science Foundation of China through Grant No. 11075020 and the SKPBRC through Grant No. 2011CB921503. Q.-S. T. acknowledges the china Postdoctoral Science Foundation through Grant No. 2013M541766.

APPENDIX

Since we consider the atoms are trapped in a symmetric double well, we have $\omega_L = \omega_R$, and $U_{LL} = U_{RR}$. By setting the resonant laser excitation $\Delta = 0$, the Hamiltonian (1) reduces to

$$\hat{H} = (\omega_L - U_{LL}/2)(\hat{a}_L^\dagger \hat{a}_L + \hat{a}_R^\dagger \hat{a}_R) + \frac{U_{LL}}{2}\hat{a}_L^\dagger \hat{a}_L \hat{a}_L^\dagger \hat{a}_L + \frac{U_{LL}}{2}\hat{a}_R^\dagger \hat{a}_R \hat{a}_R^\dagger \hat{a}_R + \frac{v}{2}(\hat{a}_L^\dagger \hat{a}_R + \hat{a}_R^\dagger \hat{a}_L). \tag{A1}$$

Since the total number of the system $\hat{N} = \hat{a}_L^\dagger \hat{a}_L + \hat{a}_R^\dagger \hat{a}_R$ is conserved, the first term of the Hamiltonian is a constant and can be neglected. Adding a constant term $-\hat{N}^2 U_{LL}/4$ to Eq. (A1), we get

$$\begin{aligned}\hat{H} &= \frac{U_{LL}}{2}(\hat{a}_L^\dagger \hat{a}_L \hat{a}_L^\dagger \hat{a}_L + \hat{a}_R^\dagger \hat{a}_R \hat{a}_R^\dagger \hat{a}_R) \\ &\quad - \frac{U_{LL}}{4}(\hat{a}_L^\dagger \hat{a}_L + \hat{a}_R^\dagger \hat{a}_R)^2 + \frac{v}{2}(\hat{a}_L^\dagger \hat{a}_R + \hat{a}_R^\dagger \hat{a}_L) \\ &= \frac{U_{LL}}{4}(\hat{a}_R^\dagger \hat{a}_R - \hat{a}_L^\dagger \hat{a}_L)^2 + \frac{v}{2}(\hat{a}_L^\dagger \hat{a}_R + \hat{a}_R^\dagger \hat{a}_L).\end{aligned} \tag{A2}$$

[1] G. J. Milburn, J. Corney, E. M. Wright, and D. F. Walls, Phys. Rev. A **55**, 4318 (1997).
[2] A. Smerzi, S. Fantoni, S. Giovanazzi, and S. R. Shenoy, Phys. Rev. Lett. **79**, 4950 (1997).
[3] S. Raghavan, A. Smerzi, S. Fantoni, and S. R. Shenoy, Phys. Rev. A **59**, 620 (1999).
[4] S. Raghavan, A. Smerzi, and V. M. Kenkre, Phys. Rev. A **60**, R1787 (1999).
[5] M. Albiez, R. Gati, Jonas Fölling, S. Hunsmann, M. Cristiani, and M. K. Oberthaler, Phys. Rev. Lett. **95**, 010402 (2005).
[6] L. Salasnich, Phys. Rev. A **61**, 015601 (1999).
[7] M. Grifoni and P. Hanggi, Phys. Rep. **304**, 229 (1998).
[8] M. H. Anderson, J. R. Ensher, M. R. Matthews, C. E. Wieman, and E. A. Cornell, Science **269**, 198 (1995).
[9] K. B. Davis, M.-O. Mewes, M. R. Andrews, N. J. van Druten, D. S. Durfee, D. M. Kurn, and W. Ketterle, Phys. Rev. Lett. **75**, 3969 (1995).
[10] C. C. Bradley, C. A. Sackett, J. J. Tollett, and R. G. Hulet, Phys. Rev. Lett. **75**, 1687 (1995).
[11] Franco Dalfovo, Stefano Giorgini, L. P. Pitaevskii, and S. Stringari, Rev. Mod. Phys. **71**, 463 (1999).
[12] G. F. Wang, L. B. Fu, and J. Liu, Phys. Rev. A **73**, 013619 (2006).
[13] M. J. Steel and M. J. Collett, Phys. Rev. A **57**, 2920 (1998).
[14] J. I. Cirac, M. Lewenstein, K. Molmer, and P. Zoller, Phys. Rev. A **57**, 1208 (1998).
[15] W. D. Li and J. Liu, Phys. Rev. A **74**, 063613 (2006).
[16] S. Kohler and F. Sols, Phys. Rev. Lett. **89**, 060403 (2002).
[17] L. B. Fu and J. Liu, Phys. Rev. A **74**, 063614 (2006).
[18] B. B. Wang, P. M. Fu, J. Liu, and B. Wu, Phys. Rev. A **74**, 063610 (2006).
[19] Y. Shin, M. Saba, T. A. Pasquini, W. Ketterle, D. E. Pritchard, and A. E. Leanhardt, Phys. Rev. Lett. **92**, 050405 (2004).
[20] J. M. Choi, G. N. Kim, and D. Cho, Phys. Rev. A **77**, 010501(R) (2008).
[21] F. Kh. Abdullaev and R. A. Kraenkel, Phys. Rev. A. **62**, 023613 (2000).
[22] Jie Liu, Biao Wu, and Qian Niu, Phys. Rev. Lett. **90**, 170404 (2003).
[23] Jie Liu, Libin Fu, Bi-Yiao Ou, Shi-Gang Chen, Dae-Il Choi, Biao Wu, and Qian Niu, Phys. Rev. A **66**, 023404 (2002).
[24] A. J. Ferris and M. J. Davis, New J. Phys. **12**, 055024 (2010).
[25] Sebastian Wüster, B. J. Dabrowska-Wüster, and Matthew J. Davis, Phys. Rev. Lett. **109**, 080401 (2012).
[26] Jacopo Sabbatini, Wojciech H. Zurek, and Matthew J. Davis, Phys. Rev. Lett. **107**, 230402 (2011).
[27] Andrew J. Ferris, Murray K. Olsen, and Matthew J. Davis, Phys. Rev. A **79**, 043634 (2009).
[28] T. J. Haigh, A. J. Ferris, and M. K. Olsen, Opt. Commun. **283**, 3540 (2010).
[29] S. Giovanazzi, A. Smerzi, and S. Fantoni, Phys. Rev. Lett. **84**, 4521 (2000).
[30] S. Choi and N. P. Bigelow, Phys. Rev. A **72**, 033612 (2005).
[31] Li-Hua Lu and You-Quan Li, Phys. Rev. A **80**, 033619 (2009).
[32] J. Ruostekoski and D. F. Walls, Phys. Rev. A **58**, R50 (1998).
[33] L. Pitaevskii and S. Stringari, Phys. Rev. Lett. **87**, 180402 (2001).
[34] Yajiang Hao and Qiang Gu, Phys. Rev. A **83**, 043620 (2011).
[35] Q. Gu and H. Qiu, Phys. Rev. Lett. **98**, 200401 (2007).
[36] K. Stiebler, B. Gertjerenken, N. Teichmann, and C. Weiss, J. Phys. B: At., Mol. Opt. Phys. **44**, 055301 (2011).
[37] D. Witthaut, F. Trimborn, H. Hennig, G. Kordas, T. Geisel, and S. Wimberger, Phys. Rev. A **83**, 063608 (2011).
[38] I. G. Savenko, T. C. H. Liew, and I. A. Shelykh, Phys. Rev. Lett. **110**, 127402 (2013).
[39] Y. Li, Y. Castin, and A. Sinatra, Phys. Rev. Lett. **100**, 210401 (2008).
[40] E. Boukobza, M. Chuchem, D. Cohen, and A. Vardi, Phys. Rev. Lett. **102**, 180403 (2009).
[41] Y. Khodorkovsky, G. Kurizki, and A. Vardi, Phys. Rev. Lett. **100**, 220403 (2008).
[42] Y. Khodorkovsky, G. Kurizki, and A. Vardi, Phys. Rev. A **80**, 023609 (2009).
[43] Y. C. Liu, G. R. Jin, and L. You, Phys. Rev. A **82**, 045601 (2010).
[44] R. Gati, B. Hemmerling, J. Fölling, M. Albiez, and M. K. Oberthaler, Phys. Rev. Lett. **96**, 130404 (2006).
[45] R. Gati, J. Estve, B. Hemmerling, T. B. Ottenstein, J. Appmeier, A. Weller, and M. K. Oberthaler, New J. Phys. **8**, 189 (2006).
[46] D. Witthaut, F. Trimborn, and S. Wimberger, Phys. Rev. Lett. **101**, 200402 (2008).
[47] D. Witthaut, F. Trimborn, and S. Wimberger, Phys. Rev. A **79**, 033621 (2009).
[48] D. A. R. Dalvit, J. Dziarmaga, and W. H. Zurek, Phys. Rev. A **62**, 013607 (2000).
[49] P. J. Y. Louis, P. M. R. Brydon, and C. M. Savage, Phys. Rev. A **64**, 053613 (2001).
[50] A. Micheli, D. Jaksch, J. I. Cirac, and P. Zoller, Phys. Rev. A **67**, 013607 (2003).
[51] W. Wang, L. B. Fu, and X. X. Yi, Phys. Rev. A **75**, 045601 (2007).
[52] M. Holthaus and S. Stenholm, Eur. Phys. J. B **20**, 451 (2001).